



Article submitted to journal

Subject Areas:

deep learning, applied mathematics, thermodynamics

Keywords:

data-driven discovery, physics-informed neural networks, GENERIC formalism, interpretable scientific machine learning

Author for correspondence:

Yeonjong Shin

e-mail: yeonjong_shin@brown.edu

GFINNs: GENERIC Formalism Informed Neural Networks for Deterministic and Stochastic Dynamical Systems

Zhen Zhang¹, Yeonjong Shin¹ and George Em Karniadakis^{1,2}

¹ Division of Applied Mathematics, and ² School of Engineering, Brown University, Providence, RI, 02912, USA

We propose the GENERIC formalism informed neural networks (GFINNs) that obey the symmetric degeneracy conditions of the GENERIC formalism. GFINNs comprise two modules, each of which contains two components. We model each component using a neural network whose architecture is designed to satisfy the required conditions. The component-wise architecture design provides flexible ways of leveraging available physics information into neural networks. We prove theoretically that GFINNs are sufficiently expressive to learn the underlying equations, hence establishing the universal approximation theorem. We demonstrate the performance of GFINNs in three simulation problems: gas containers exchanging heat and volume, thermoelastic double pendulum and the Langevin dynamics. In all the examples, GFINNs outperform existing methods, hence demonstrating good accuracy in predictions for both deterministic and stochastic systems.

1. Introduction

The discovery of governing equations for dynamical systems from observed data is a longstanding scientific endeavor [1–3]. The so-called data-driven discovery dated back to Kepler refers to scientific methods that extract important features from data and either approximate or identify governing equations by means of (parameterized) function classes. With the recent advancement in deep learning, neural network classes have been popularly employed in modelling and simulations and have demonstrated some promising

© The Authors. Published by the Royal Society under the terms of the Creative Commons Attribution License <http://creativecommons.org/licenses/by/4.0/>, which permits unrestricted use, provided the original author and source are credited.

empirical results [4–9].

The data-driven discovery may be classified into two major approaches. One is the pure data-driven methods [10,11] which model governing equations using neural networks that are trained to fit observed data *without physics*. This approach could provide a neural network model that mimics training trajectories, particularly when no physics but a large amount of data are available. However, it is likely that the learned models do not generalize well on the region where training data are scarce or even do not exist. The other is the physics-informed data-driven approach, which aims to model governing equations by *embedding principles of physics into neural networks* together with data. By exploiting physics, it was empirically observed that the amount of data needed to get good performance is much less than those of the pure data-driven methods, and the learned model is stable and generalizes well. Typically, the physics are imposed on neural networks by means of either soft or hard constraints. The use of soft constraints introduces regularization terms in an associated loss function that penalize and generalize neural networks that do not obey the physics [12–15]. The hope is that neural networks approximately follow the physics after training. The hard constraints are typically imposed by designing proper neural network architectures that obey the underlying principles without optimization processes [16,17], yet maintain sufficient expressivity so that governing equations can be learned from data. This is the approach we follow in the current paper. A schematic diagram of the classification of the data-driven discovery is given in Figure 1.

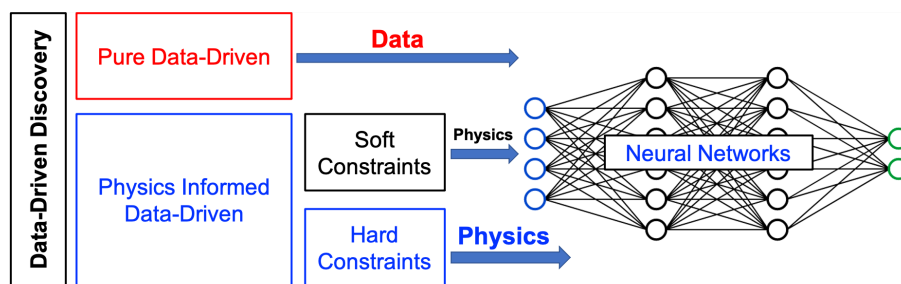


Figure 1. A schematic diagram showing the major three approaches in the data-driven discovery of dynamical systems. One is the pure data-driven approach. The other two are the physics informed data-driven approach. The second one is based on soft constraints imposed in an associated loss function. The third one directly imposes the underlying physics into neural networks by designing novel network architectures.

Among many principles of physics, we consider the General Equation for Non-Equilibrium Reversible-Irreversible Coupling (GENERIC) formalism [18–20]. GENERIC provides a general mathematical framework describing states beyond equilibrium of a dynamical system [20], which involves two separate generators for the reversible and irreversible dynamics. These generators are required to satisfy some symmetry and degeneracy conditions, which constitute a key feature of the GENERIC structure. These conditions are often interpreted as the first and second principles of thermodynamics, which further can be expressed in the language of linear algebra.

Our goal is to embed the GENERIC structure directly into neural networks, yet to maintain sufficient expressivity. By leveraging the level of prior physics information under the GENERIC framework, we propose a systematical approach in designing neural network modules.

In the case where either one or all generators are known *a priori*, we design neural network models for either energy or entropy or both by exploiting certain properties of the generators. Due to the multiplicative structure of the gradient of neural networks, care needs to be taken into the input layer in order to meet the degeneracy conditions. We thus introduce a transformation in the first layer, which roughly speaking, projects input into a proper low-dimensional space on which the degeneracy conditions hold. On the other hand, if no prior information is available, we model

generators by neural networks whose architectures are motivated by the spectral decomposition of matrix [21]. In any cases, the proposed neural network models obey the required constraints exactly. We refer to our neural network models as the GENERIC formalism informed neural networks (GFINNs).

Furthermore, we prove the universal approximation theorem for GFINNs under some assumptions. Altogether, GFINNs not only obey the required GENERIC conditions, but also are sufficiently expressive in learning the underlying physical quantities and generators. We demonstrate the performance of GFINNs on several tasks including double pendulums, gas containers and stochastic differential equations. We found that GFINNs outperform the existing network architectures [15,22,23] in all the tests we considered.

There are two existing works that have attempted to embed the GENERIC formalism into neural networks. [15] proposed structure preserving neural networks (SPNNs), which aim to learn the physical quantities assuming both generators are known. The degeneracy requirements are softly constrained in the loss function, which may cause violation of the degeneracy conditions even after training. [23] proposed the GENERIC neural ordinary differential equations (GNODEs), which satisfy the required conditions by suitable parameterization of bracket structure, however, no universal approximation theorem has been proven.

The rest of the paper is organized as follows. Upon introducing the problem setup and some preliminaries in Section 2, the GENERIC formalism informed neural networks (GFINNs) are presented in Section 3 along with the universal approximation theorem. Numerical examples are provided in Section 4, demonstrating the effectiveness of GFINNs against other methods.

2. Problem Setup

We consider the problem of learning an autonomous dynamical system that can be expressed in the following form:

$$\dot{z}(t) = F(z), \quad z \in \Omega \subset \mathbb{R}^d, \quad t \in [0, T], \quad z(0) = z_0, \quad (2.1)$$

where t refers to the time coordinates and $F(z)$ is the unknown vector-valued field function.

With the goal of approximating $F(z)$ through data, we employ a neural network $F_{\text{NN}}(z; \theta)$ whose parameters are determined so that the trajectories generated from the resulting dynamics $\dot{z}(t) = F_{\text{NN}}(z; \theta)$ are close to the observed trajectory data. More precisely, let N_{traj} be the number of observed trajectories. Let T be the number of time-steps and t_j be the j -th time stamp, which we set them equal for all trajectories for the sake of notational simplicity. Let $z(t; z_0)$ be the state variable at time t whose value at t_0 is z_0 . Then, the k -th trajectory is written as $\{t_j, z(t_j; z_0^{(k)})\}_{j=0}^T$. We then seek to find the optimal network parameters that minimize the loss function defined by

$$\mathcal{L}(\theta) = \frac{1}{N_{\text{traj}}} \sum_{k=1}^{N_{\text{traj}}} \frac{1}{T} \sum_{j=1}^T \left\| z_{\text{NN}}^\theta(t_j; z_0^{(k)}) - z(t_j; z_0^{(k)}) \right\|^2. \quad (2.2)$$

Here $z_{\text{NN}}^\theta(t_j; z_0^{(k)})$ is computed by applying a numerical integrator [24] (e.g., Runge–Kutta methods) to the equation $\dot{z}(t) = F_{\text{NN}}(z; \theta)$ starting at $z(t_{j-1}; z_0^{(k)})$; $\|\cdot\|$ is the standard Euclidean norm. Typically, gradient-based optimization methods are used to solve this minimization problem.

If no physics is involved, the above gives a general description of the pure data-driven approach. If some principles of physics are known, the physics-informed data-driven approach aims to embed the available physics into neural networks. There are two typical ways of doing the embedding. One is to add regularization terms to the loss (2.2) that penalize F_{NN} that do not follow the physics. The other is to devise a network architecture so that F_{NN} obeys the available physics for any θ and the optimal parameters are then found by minimizing the same loss (2.2).

(a) The GENERIC formalism

The General Equation for Non-Equilibrium Reversible-Irreversible Coupling (GENERIC) formalism provides a general mathematical framework describing *beyond-equilibrium* thermodynamic systems [20] including both conservative and dissipative systems. As a consequence, any system described by Hamilton's equation or Poisson's equation can be written in the GENERIC formalism, as follows:

$$\begin{aligned} \dot{z}(t) &= L(z) \frac{\partial E}{\partial z}(z) + M(z) \frac{\partial S}{\partial z}(z), \\ \text{subject to } L(z) \frac{\partial S}{\partial z}(z) &= M(z) \frac{\partial E}{\partial z}(z) = \mathbf{0}, \\ L(z) &\text{ is skew-symmetric, i.e., } L(z) = -L(z)^\top \\ M(z) &\text{ is symmetric positive semi-definite.} \end{aligned} \quad (2.3)$$

The term $L \frac{\partial E}{\partial z}$ accounts for all the reversible (non-dissipative) phenomena of the system. In the classical mechanics, this term is equivalent to Hamilton and Poisson's equations of motion. The operator L is called the Poisson matrix and is required to be skew-symmetric. The term $M \frac{\partial S}{\partial z}$ accounts for the irreversible (dissipative) material properties of the system. This term was motivated by the Ginzburg-Landau equation, which can be used to describe critical dynamics of spatially extended systems. The operator M is called the friction matrix and is required to be symmetric positive semi-definite. $E(z)$ and $S(z)$ are the system's total energy and entropy, respectively. Under this framework, it can be checked that the energy of the system is conserved and the entropy of the system monotonically increases with respect to time, i.e., $\frac{dE(z(t))}{dt} = 0$ and $\frac{dS(z(t))}{dt} \geq 0$, corresponding to the first and second laws of thermodynamics, respectively.

(b) Deep Neural Networks

We employ deep neural networks as the basic components in our surrogate modellings for L, M, E, S . For simplicity of discussion, we shall focus on feed-forward neural networks throughout this work, while any types of neural networks (e.g., ResNet) can easily be used in place of the feed-forward networks without difficulties.

A L -layer feed-forward neural network $f: \mathbb{R}^{d_{\text{in}}} \rightarrow \mathbb{R}^{d_{\text{out}}}$ is defined by $f(x) = z^{L+1}(x)$ where z^{L+1} is constructed recursively according to

$$z^\ell(x) = W^\ell \phi(z^{\ell-1}(x)) + b^\ell, \quad 1 < \ell \leq L + 1,$$

starting with $z^1(x) = W^1 x + b^1$. Here, $W^\ell \in \mathbb{R}^{n_\ell \times n_{\ell-1}}$ is the weight matrix and $b^\ell \in \mathbb{R}^{n_\ell}$ is the bias vector in the ℓ -th layer, where we set $n_0 = d_{\text{in}} = d$ and $n_L = d_{\text{out}}$. $\phi(x)$ is a nonlinear activation function that is applied element-wise. The activation function is assumed to have certain properties so that the universal approximation theorem holds [25–27]. The collection of all weights and biases of the network is denoted by $\theta = \{(W^1, b^1), \dots, (W^L, b^L)\}$. We note that a neural network can be a matrix-valued function by converting the output to a matrix of proper size.

Let $f(x; \theta): \mathbb{R}^d \rightarrow \mathbb{R}$ be a L -layer neural network and $g: \mathbb{R}^d \rightarrow \mathbb{R}^d$ be a differentiable function. The gradient of $(f \circ g)(x) = f(g(x))$ with respect to x is given by

$$\nabla_x f(g(x); \theta) = \mathbf{J}g(x)^\top \left(W^L D_{L-1} \cdots W^2 D_1 W^1 \right)^\top = \mathbf{J}g(x)^\top \nabla_x f \circ g(x), \quad (2.4)$$

where D_j is a diagonal matrix whose (i, i) -entry is $\phi'(z_i^j(g(x)))$ for $1 \leq j < L$ and $1 \leq i \leq n_j$, and $\mathbf{J}g(x)$ is the Jacobian of g at x . A key observation is that $\nabla_x f(g(x); \theta)$ belongs to the row space of $\mathbf{J}g(x)$ due to the multiplicative structure. We refer to the equation (2.4) as the multiplicative structure of the gradient of neural networks.

3. GENERIC Formalism Informed Neural Networks

Our goal is to design neural network architectures that satisfy the symmetry and degeneracy conditions of (2.3), yet are sufficiently expressive to learn the underlying dynamics from data. Also, we want the proposed neural networks to be easily adopted when some prior physics is available (in terms of the GENERIC).

Since the GENERIC formalism comprises two orthogonal modules, each of which contains two components, we model each component using neural networks that satisfy the required conditions. The component-wise design not only allows the flexibility in incorporating prior physics (if any) but also results in a general framework of neural network modellings for the GENERIC formalism. Here, prior physics implies a scenario where one or more is known among L, M, E, S . Although many possibilities can be discussed, for the sake of simplicity, we focus on the following scenarios:

- Case 1: L and M are known. The goal is to approximate E and S .
- Case 2a: E and S are unknown. The goal is to approximate L and M .
- Case 2b: L, M, E, S are unknown. The goal is to approximate L, M, E, S .

All other scenarios can be handled without difficulties. The schematic of the proposed framework is shown in Figure 2.

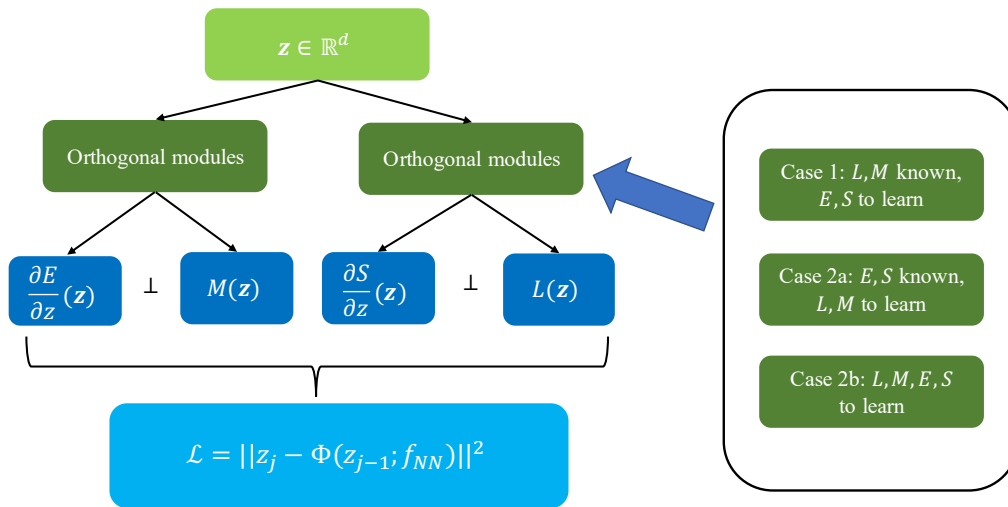


Figure 2. Architecture of GFINNs. GFINNs can be seen as a neural network framework, which automatically satisfies the laws of thermodynamics. The design of GFINNs follows the GENERIC formalism since we parameterize the (matrix-valued) functions L, M, E, S as orthogonal neural network modules, which satisfy the consistency condition and structural condition in Eq. 2.3. We propose different architectures, which can incorporate different physical information including the knowledge of L, M or the knowledge of E, S .

Requiring only the conditions of (2.3) can be done quite easily, while care is needed to ensure expressivity. We illustrate this through the following example. Let

$$L(z) = \begin{bmatrix} 0 & \ell(z) & 0 & 0 \\ -\ell(z) & 0 & 0 & 0 \\ 0 & 0 & 0 & 0 \\ 0 & 0 & 0 & 0 \end{bmatrix}, \quad \ell(z) \neq 0.$$

Suppose the goal is to construct a proper neural network S_{NN} satisfying $L(\mathbf{z})\nabla S_{\text{NN}}(\mathbf{z})\neq \mathbf{0}$. Since $\text{null}(L(\mathbf{z})) = \text{span}\{e_3, e_4\}$, where $e_3 = [0, 1, 0]^\top$ and $e_4 = [0, 0, 1]^\top$, we have infinitely many choices for S_{NN} that satisfy the condition. For example, if S_{NN} is any smooth function of z_3 and does not depend on the other variables, the required condition is trivially satisfied. However, this class of functions does not capture the potential dependence of z_4 , so that a sufficient expressiveness is not guaranteed. Similarly, if S were given and the goal was to model a skew-symmetric matrix L_{NN} that satisfies $L_{\text{NN}}(\mathbf{z})\nabla S(\mathbf{z})\neq \mathbf{0}$, there are also infinitely many choices for L_{NN} that satisfy the required condition, yet not all of them are sufficiently expressive.

For ease of discussion, in what follows, we denote a generic matrix function by A representing either L or M , and a generic scalar function by G representing either S or E . Also, the subscript (G_{NN} or A_{NN}) indicates the neural network model for the target quantity (G or A). Next, we discuss how to construct neural networks for modelling each component and present the corresponding universal approximation theorem under some assumptions.

(a) Case 1: L and M are known and E and S are unknown

We consider the case where L and M are known, yet E and S are unknown. Since the two generators are known, one might attempt to model ∇E and ∇S directly using neural networks following the pure data-driven approach [10]. However, since all vector functions are not gradient of a scalar function, we construct neural networks for E and S and compute their gradients by automatic differentiation that can be implemented by well-established programming packages e.g., Pytorch [28] and Tensorflow [29]. Furthermore, by construction, this approach allows one to not only predict the solution trajectories but also discover physical quantities (energy and entropy) from data.

Since we have multiple goals to achieve, several challenges arise in developing neural network architectures with the desired properties. First of all, since we model G (i.e., E or S) instead of ∇G , we need to properly control the gradient of neural networks so that the degeneracy condition of (2.3) holds. Motivated by the multiplicative structure (2.4), we introduce a tailored projection-like transformation \mathcal{P}_A in the very first layer of neural networks, which ensures the degeneracy condition under some assumptions. It is the transformation \mathcal{P}_A that constitutes a core element in the network architecture for G (either E and S) assuming A is known.

As a preparation for introducing the transformation \mathcal{P}_A and also for the universal approximation theorem, we make a couple of basic assumptions on A , which will be justified in all the examples later.

Assumption 1. Let $A(\mathbf{z})$ be a $d \times d$ matrix-valued function defined on $\Omega \subset \mathbb{R}^d$. Let $q_A^j(\mathbf{z})$, $j = 1, \dots, n_A$, be an orthonormal basis of $\ker A(\mathbf{z}) = \{y \in \mathbb{R}^d : A(\mathbf{z})y = \mathbf{0}\}$ whose rank is n_A . We assume that

- (i) $\ker A(\mathbf{z})$ has constant rank $n_A \in \{1, \dots, d-1\}$ in Ω .
- (ii) $\ker_{\text{inv}} A(\mathbf{z}) = \text{span}\{q_A^j : 1 \leq j \leq \tilde{n}_A\}$ is the largest subspace of $\ker A(\mathbf{z})$ whose rank is \tilde{n}_A which is also constant on Ω such that $q_A^j(\mathbf{z})$, $j = 1, \dots, \tilde{n}_A$, satisfy

$$\text{range}(\mathbf{J}q_A^j(\mathbf{z})^\top) \subset \ker A(\mathbf{z}), \quad (3.1)$$

where $\mathbf{J}q(\mathbf{z})$ is the Jacobian matrix of $q(\mathbf{z})$.

Assumption 2. Let $A : \mathbb{R}^d \rightarrow \mathbb{R}^{d \times d}$ be a matrix-valued function satisfying Assumption 1 and let $\hat{n}_A = n_A - \tilde{n}_A$. There exist real-valued differentiable functions $F_A^j(\mathbf{z})$, $j = 1, \dots, \hat{n}_A$, on Ω , satisfying

$$\text{span}\{\nabla F_A^j(\mathbf{z}) : j = 1, \dots, \hat{n}_A\} \oplus \ker_{\text{inv}} A(\mathbf{z}) = \ker A(\mathbf{z}). \quad (3.2)$$

The degeneracy conditions of (2.3), if it is interpreted in terms of linear algebra, means that ∇G belongs to the kernel of A . Since $\ker A(\mathbf{z})$ depends on \mathbf{z} , Assumption 1(i) basically allows us

to work on the fixed number of basis. This is a typical assumption made in order to make analysis go through, which is also used in [30] dated back in 1970s. Assumption 1(ii) and 2 decompose $\mathfrak{K} \setminus A(z)$ into two subspaces, one of which satisfies the invariance under differentiation in the sense of (3.1). The other subspace from Assumption 2 provides the key information on how to keep ∇G_{NN} in the kernel of $A(z)$ as a function of z . The existence of the functions F_A^j plays a key role in defining the transformation \mathcal{P}_A .

With these assumptions, we define a transformation \mathcal{P}_A as follows. From Assumption 1, let $\tilde{Q}_A(z) = [q_A^1(z), \dots, q_A^{\tilde{n}_A}(z)]$. From Assumption 2, let $F_A(z) = [F_A^1(z), \dots, F_A^{\tilde{n}_A}(z)]^\top$. Define the transformation $\mathcal{P}_A : \mathbb{R}^d \rightarrow \mathbb{R}^{n_A}$ by

$$\mathcal{P}_A(z) = [\tilde{Q}_A^\top(z)z; F_A(z)] \in \mathbb{R}^{n_A}. \quad (3.3)$$

The first \tilde{n}_A components of $\mathcal{P}_A(z)$ is the orthogonal projection coefficients of z onto $\mathfrak{K} \setminus_{\text{inv}} A(z)$ and the remaining components are the functions from Assumption 2. The output of \mathcal{P}_A is n_A -dimensional vector resulting in a dimension reduction from d to n_A .

We are now in a position to present our neural networks for $G(z)$ (either energy $E(z)$ or entropy $S(z)$). For neural networks $f(z; \theta) : \mathbb{R}^d \rightarrow \mathbb{R}$, we define

$$G_{\text{NN}}(z; \theta_A) = f(\mathcal{P}_A(z); \theta_A). \quad (3.4)$$

It then follows from the multiplicative structure (2.4) and the properties of the transformation (3.3) stemmed from Assumptions 1 and 2 that any G_{NN} of the form (3.4) satisfies $A(z)\nabla G(z) = \mathbf{0}$ for all $z \in \Omega$. We note that in general, the functions from Assumption 2 may not be readily available. However, in Propositions 1 and 2, we show that F_A can be identified by extracting relevant components from the basis of $\mathfrak{K} \setminus A(z)$ and then applying indefinite integration.

The remaining goal is to show the expressivity of the proposed neural network architecture (3.4). In order to show the universal approximation theorem, an appropriate function class should be chosen in the first place on which we show the universality. Since the target function G satisfying the degeneracy condition of (2.3) depends highly on the properties of the kernel of an operator A , a general function class requires some detailed characterizations of $\mathfrak{K} \setminus A(z)$. We thus confine ourselves to the function class \mathcal{F}_A characterized by the transformation operator \mathcal{P}_A together with the multiplicative structure (2.4).

Definition 1. Let $A : \mathbb{R}^d \rightarrow \mathbb{R}^{d \times d}$ be a matrix-valued function satisfying Assumptions 1 and 2. Let \mathcal{F}_A be the collection of differentiable functions G defined on $\Omega \subset \mathbb{R}^d$ whose gradient satisfies

$$\nabla G(z) \in \mathbf{J}\mathcal{P}_A(z)^\top \mathbf{c}_A \circ \mathcal{P}_A(z), \quad \forall z \in \Omega, \quad (3.5)$$

for some continuous function $\mathbf{c}_A : \mathbb{R}^{n_A} \rightarrow \mathbb{R}^{n_A}$.

The function class \mathcal{F}_A of Definition 3.5 depends crucially on A . For example, as shown in Corollary 1, if A is constant, \mathcal{F}_A contains all the continuously differentiable functions G that satisfy $\nabla G \in \mathfrak{K} \setminus A(z)$.

Corollary 1. Suppose A is constant. Then, \mathcal{F}_A is the class $C^1(\Omega)$ that consists of all differentiable functions whose gradient lies in $\mathfrak{K} \setminus A$ and continuous on Ω .

Proof. Since A is constant, so is Q . Also $n = n_A \cong \tilde{n}_A \oplus \emptyset$, $\mathcal{P}_A(z) = Q^\top z$ and $(\mathbf{J}\mathcal{P}_A(z))^\top = Q$. Let $\mathfrak{G}(\xi) = G(Q\xi)$ where $\xi \in \mathbb{R}^n$. It then follows from $\nabla G(z) = Q\nabla_\xi G(Q\xi)|_{\xi=Q^\top z}$ that $\nabla G(z) = Q\nabla_\xi \mathfrak{G}(\xi)|_{\xi=Q^\top z} = Q\nabla_\xi \mathfrak{G} \circ \mathcal{P}_A(z)$. By letting $\mathbf{c}_A(\xi) = \nabla_\xi \mathfrak{G}(\xi)$, the proof is completed. \square

With the target function class being defined, we now show that the proposed neural network G_{NN} defined in (3.4) is universal for the function class \mathcal{F}_A .

Theorem 1. Suppose $A(\mathbf{z})$ is a $d \times d$ -matrix-valued function on $\Omega \subset \mathbb{R}^d$ satisfying Assumptions 1 and 2. For any $G(\mathbf{z}) \in \mathcal{F}_A$ defined as in (3.5) and a small $\epsilon > 0$, there exists a neural network model $G_{\text{NN}}(\mathbf{z})$ defined as in (3.4) such that

$$\forall \mathbf{z} \in \Omega \quad \|\nabla G(\mathbf{z}) - \nabla G_{\text{NN}}(\mathbf{z})\| < \epsilon,$$

and $A(\mathbf{z}) \frac{\partial G_{\text{NN}}}{\partial \mathbf{z}}(\mathbf{z}) = \mathbf{0}$ for all $\mathbf{z} \in \Omega$.

Proof. Note that $\frac{\partial G_{\text{NN}}}{\partial \mathbf{z}}(\mathbf{z}) \in \mathbf{J}\mathcal{P}_A(\mathbf{z})^\top \nabla f \circ \mathcal{P}_A(\mathbf{z})$. Since $G^* \in \mathcal{F}_A$, there exists a continuous function \mathbf{c}_A^* such that the gradient of G^* is expressed as $\nabla G^*(\mathbf{z}) \in \mathbf{J}\mathcal{P}_A(\mathbf{z})^\top \mathbf{c}_A^* \circ \mathcal{P}_A(\mathbf{z})$. Since $\mathbf{J}\mathcal{P}_A(\mathbf{z})$ is full rank on Ω , by invoking the universal approximation theorem of neural networks (e.g., [26,31]), for any sufficiently small $\epsilon > 0$, there exists a neural network f satisfying $\forall \mathbf{z} \in \Omega \quad \|\nabla f \circ \mathcal{P}_A(\mathbf{z}) - \mathbf{c}_A^* \circ \mathcal{P}_A(\mathbf{z})\| < \epsilon$, which completes the proof. \square

An explicit neural network architecture in terms of width and depth may be given from existing works, however, we simply rely on the well-established universal approximation theorem for neural networks [25–27,31].

The considered function class \mathcal{F}_A from Definition 3.5 may be too restricted to cover more general functions. However, in all the examples of Section 4, we show that all the assumptions hold and the underlying energy E and entropy S functions belong to the function classes \mathcal{F}_M and \mathcal{F}_L , respectively.

(b) Case 2: L , M , E and S are unknown

We consider only Case 2b where all the quantities (L , M , E , S) are unknown, since Case 2a is easily handled by letting $G_{\text{NN}} = G$.

In Case 2, a scalar function G is modelled by a standard neural network unless it is known a priori. It then suffices to construct a matrix-valued neural network A_{NN} from G_{NN} that satisfies both the symmetry and the degeneracy conditions. Unlike Case 1, we do not need to control the gradient of G_{NN} to be in $\mathbf{k} \quad A(\mathbf{z})$. Rather, we design A_{NN} to satisfy $\nabla G_{\text{NN}} \in \mathbf{k} \quad A_{\text{NN}}(\mathbf{z})$. It turns out that one can easily adopt this property into neural network architectures by exploiting skew-symmetric matrices.

Lemma 1. For $j = 1, \dots, K$, let S_j be a skew-symmetric matrix of size $d \times d$. For a differentiable scalar function $g(x) : \mathbb{R}^d \rightarrow \mathbb{R}$, let $Q_g(x) \in \mathbb{R}^{K \times d}$ be a matrix-valued function whose j -th row is defined to be $(S_j \nabla g(x))^\top$. Then, $Q_g(x) \nabla g(x) = \mathbf{0}$ for all $x \in \mathbb{R}^d$.

Proof. The proof readily follows from the fact that for any $y \in \mathbb{R}^d$, $y^\top S_j y = 0$ since S_j is skew-symmetric. \square

For a neural network G_{NN} , let $Q_{G_{\text{NN}}}(\mathbf{z})$ be the matrix function defined through K skew-symmetric matrices as in Lemma 1, which are trainable parameters. Motivated by the spectral decomposition of either skew-symmetric or symmetric positive semi-definite matrix, we propose to model A by

$$A_{\text{NN}}(\mathbf{z}) \in Q_{G_{\text{NN}}}(\mathbf{z})^\top B_{\text{NN}}^A(\mathbf{z}) Q_{G_{\text{NN}}}(\mathbf{z}), \quad (3.6)$$

where $B_{\text{NN}}^A(\mathbf{z})$ is skew-symmetric if $A = L$ and is symmetric positive semi-definite if $A = M$ that is modelled by another neural network different from G_{NN} . In particular, we use two triangular matrix-valued neural networks $T_L(\mathbf{z})$ and $T_M(\mathbf{z})$ and set

$$B_{\text{NN}}^L(\mathbf{z}) \in T_L(\mathbf{z})^\top - T_L(\mathbf{z}), \quad B_{\text{NN}}^M(\mathbf{z}) \in T_M(\mathbf{z})^\top T_M(\mathbf{z}). \quad (3.7)$$

By construction, the symmetry and degeneracy conditions of (2.3) are automatically satisfied.

We note that if A is either skew-symmetric or symmetric positive semi-definite, the spectral decomposition reads $A = Q^\top \Lambda Q$, where Q is orthogonal and Λ is either skew-symmetric or

diagonal. The network architecture of (3.6) has a similar structure of that of the spectral decomposition, yet, neither $Q_{G_{NN}}$ is orthogonal nor B_{NN}^A is the eigenvalue matrix. Since $Q_{G_{NN}}$ is a matrix of size $K \times d$, the rank of A_{NN} is at most in $\{K, d\}$. Hence, K is assumed to be greater than or equal to the rank of A .

Owing to the universal approximation theorem [25,27] of neural networks, we show that the proposed neural network A_{NN} of (3.6) is sufficiently expressive enough to approximate the underlying target function A under some mild conditions.

Theorem 2. Suppose $\nabla G_{NN} = \nabla G$ is continuous on a compact set $\Omega \subset \mathbb{R}^d$, and a component of $\nabla G(\mathbf{z})$ has nonzero values in Ω . Let $A(\mathbf{z})$ be either a skew-symmetric or symmetric positive semi-definite matrix-valued continuous function satisfying $A(\mathbf{z})\nabla G(\mathbf{z}) \neq \mathbf{0}$ for all $\mathbf{z} \in \Omega$. For any $\epsilon > 0$, there exists a neural network model A_{NN} of the form (3.6) such that $\sup_{\mathbf{z} \in \Omega} \|A - A_{NN}\| < \epsilon$ and $A_{NN}(\mathbf{z})\nabla G(\mathbf{z}) = \mathbf{0}$ in Ω .

Proof. Without loss of generality, let $(\nabla G(\mathbf{z}))_1 \neq 0$ for all $\mathbf{z} \in \Omega$. Since $A\nabla G \neq \mathbf{0}$, the column space $\text{col}A(\mathbf{z})$ is spanned by at most $d - 1$ independent basis. For $k = 1, \dots, d - 1$, let P_k be a skew-symmetric matrix of size d such that $(P_k)_{1,k+1} = 1$, $(P_k)_{k+1,1} = -1$ and $(P_k)_{ij} = 0$ otherwise. Let $\tilde{q}_k(\mathbf{z}) = P_k \nabla S(\mathbf{z})$.

Claim 1. $\tilde{q}_k(\mathbf{z})$, $1 \leq k < d$, are linearly independent and

$$\text{col}(A(\mathbf{z})) \subseteq \text{span}\{\tilde{q}_k(\mathbf{z}) \mid 1 \leq k < d\}.$$

Proof of Claim. Assuming $\sum_{k=1}^{d-1} c_k \tilde{q}_k(\mathbf{z}) = \mathbf{0}$, it suffices to show $c_k = 0$ for all k . Observe that

$$\sum_{k=1}^{d-1} c_k \tilde{q}_k(\mathbf{z}) = \left[\sum_{k=1}^{d-1} c_k (\nabla G(\mathbf{z}))_{k+1} \quad -c_1 (\nabla G(\mathbf{z}))_1 \quad \cdots \quad -c_{d-1} (\nabla G(\mathbf{z}))_1 \right]^\top.$$

Since $(\nabla G(\mathbf{z}))_1 \neq 0$, $c_1 = \cdots = c_{d-1} = 0$, which proves the linearly independence. Note also that since P_k is skew-symmetric, $\langle \tilde{q}_k(\mathbf{z}), \nabla G(\mathbf{z}) \rangle = 0$ for all k . The second claim is followed from the relationship

$$\text{col}(A(\mathbf{z})) \subseteq (\text{span}\{\nabla G(\mathbf{z})\})^\perp = \text{span}\{\tilde{q}_k(\mathbf{z}) \mid 1 \leq k < d\},$$

where the equality holds because the two spaces have the same rank. \square

Note that A is either skew-symmetric or symmetric positive semi-definite of rank r with $2 \leq r < d$. We shall consider only the case when A is skew-symmetric. The other case can be proved similarly. Thus, it can be decomposed as $A(\mathbf{z}) = Q(\mathbf{z})\Lambda(\mathbf{z})Q^\top(\mathbf{z})$, where $Q(\mathbf{z})$ is a matrix of size $d \times r$ such that $Q^\top(\mathbf{z})Q(\mathbf{z}) = I \in \mathbb{R}^{r \times r}$ and $\Lambda(\mathbf{z})$ is skew-symmetric of size $r \times r$ defined by

$$(A(\mathbf{z}))_{ij} = \begin{cases} \lambda_i(\mathbf{z}) & \text{if } j = i + 1, \\ -\lambda_i(\mathbf{z}) & \text{if } j = i - 1, \\ 0 & \text{otherwise,} \end{cases}$$

where $\lambda_i(\mathbf{z}) > 0$. Thus, there exists a matrix $R(\mathbf{z}) \in \mathbb{R}^{(d-1) \times r}$ such that $Q(\mathbf{z}) = \tilde{Q}(\mathbf{z})R(\mathbf{z})$, where $\tilde{Q}(\mathbf{z}) = [q_1(\mathbf{z}), \dots, q_{d-1}(\mathbf{z})]$. Since $Q^\top(\mathbf{z})\tilde{Q}(\mathbf{z})$ is full rank and $r \leq d - 1$, a solution to $Q^\top(\mathbf{z})\tilde{Q}(\mathbf{z})R(\mathbf{z}) = I$ always exists.

Since $A(\mathbf{z})$ is continuous on $\Omega \subset \mathbb{R}^d$, so does $\tilde{\Lambda}(\mathbf{z}) = R(\mathbf{z})\Lambda(\mathbf{z})R^\top(\mathbf{z})$. From the universal approximation theorem of neural networks, there exists a skew-symmetric matrix-valued neural

network $B_{\text{NN}}^A(\mathbf{z})$ such that

$$\|(B_{\text{NN}}^A(\cdot))_{ij} - (\tilde{A}(\cdot))_{ij}\|_{C^0(\Omega)} < \frac{\epsilon}{C(d-1)r}, \quad \forall 1 \leq i < j < d, \quad (3.8)$$

where $C = \int_{\mathbf{z} \in \Omega} \|\tilde{Q}(\mathbf{z})\|^2$. Note that C is a constant that depends only on $\nabla G(\mathbf{z})$ and Ω . Therefore,

$$\begin{aligned} \|A(\mathbf{z}) - A_{\text{NN}}(\mathbf{z})\| &= \|Q(\mathbf{z})A(\mathbf{z})Q^\top(\mathbf{z}) - \tilde{Q}(\mathbf{z})B_{\text{NN}}^A(\mathbf{z})\tilde{Q}^\top(\mathbf{z})\| \\ &= \|\tilde{Q}(\mathbf{z})R(\mathbf{z})A(\mathbf{z})R^\top(\mathbf{z})\tilde{Q}^\top(\mathbf{z}) - \tilde{Q}(\mathbf{z})B_{\text{NN}}^A(\mathbf{z})\tilde{Q}^\top(\mathbf{z})\| \\ &\leq \|\tilde{Q}(\mathbf{z})\|^2 \|R(\mathbf{z})A(\mathbf{z})R^\top(\mathbf{z}) - B_{\text{NN}}^A(\mathbf{z})\|. \end{aligned}$$

Since $\|\cdot\| \leq \|\cdot\|_F$, where $\|\cdot\|_F$ is the Frobenius norm, it follows from (3.8) that $\|A(\mathbf{z}) - A_{\text{NN}}(\mathbf{z})\| \leq \epsilon$ for all $\mathbf{z} \in \Omega$, which completes the proof. \square

Assuming Case 2b, the GENERIC formalism informed neural networks (GFINNs) comprise of four neural networks: $E_{\text{NN}}, S_{\text{NN}}, B_{\text{NN}}^L, B_{\text{NN}}^M$ together with sets of trainable parameters forming skew-symmetric matrices used in $Q_{E_{\text{NN}}}$ and $Q_{S_{\text{NN}}}$. Apart from parameters for the four neural networks, the number of parameters from the skew-symmetric matrices is $2Kd(d-1)$. When the dimension d is large, the number of trainable parameters grows $\mathcal{O}(Kd^2)$, which may cause some computational challenges. If this is the case, sparse parameterization can be applied to reduce the number of parameters. For example, each skew-symmetric matrix could be sparsely parameterized by only s nonzero parameters, which reduces the number of trainable parameters from $\mathcal{O}(Kd^2)$ to $\mathcal{O}(Ks)$. A similar sparse parameterization can be applied in modelling B_{NN}^A as well.

In summary, GFINNs consist of four components, $E_{\text{NN}}, S_{\text{NN}}, L_{\text{NN}}, M_{\text{NN}}$ that form two modules; E-M module ($E_{\text{NN}}, M_{\text{NN}}$) and L-S module ($L_{\text{NN}}, S_{\text{NN}}$). When A is known, we model G using a neural network G_{NN} of the form (3.4). When G is known, we model A using a neural network A_{NN} of the form (3.6). When no physics is known, we model G using a standard neural network G_{NN} and then model A using a neural network A_{NN} of the form (3.6) with G_{NN} . As a result, we obtain a general framework of designing neural networks for the GENERIC formalism with the flexibility of incorporating available physics, thanks to the component-wise network modelling.

4. Numerical Examples

We demonstrate the performance of GFINNs on three benchmark problems. To compare against other methods, we also report the results obtained by GNODEs [23], SPNNs [15], and SDENets [22]. Implementation details can be found in Appendix A. We note that SPNNs and GNODEs can only be applied in case 1 and case 2, respectively, while GFINNs cover all the cases.

Nonuniqueness. By the multiplicative structure, the GENERIC formalism allows multiple modules resulting in the same dynamics. That is, given (E, S, L, M) , there are infinitely many $(\tilde{E}, \tilde{S}, \tilde{L}, \tilde{M})$ satisfying $\tilde{L}(\mathbf{z})\frac{\partial \tilde{E}}{\partial \mathbf{z}}(\mathbf{z}) + \tilde{M}(\mathbf{z})\frac{\partial \tilde{S}}{\partial \mathbf{z}}(\mathbf{z}) = L(\mathbf{z})\frac{\partial E}{\partial \mathbf{z}}(\mathbf{z}) + M(\mathbf{z})\frac{\partial S}{\partial \mathbf{z}}(\mathbf{z})$. As a matter of fact, if we let \tilde{G} be an affine transformation of G with a slope coefficient a , by letting $\tilde{A} = a^{-1}A$, we obtain new modules resulting in the same dynamics. Because of the nonuniqueness, the inferred quantities E_{NN} and S_{NN} may look different from the target quantities. We therefore calibrate the inferred quantities to make them look similar to the ground truth values. The calibration is done by finding aforementioned affine transformations using some target values. We apply the calibration only for the visualization purpose to demonstrate the discovery of the physical quantities by GFINNs.

GENERIC formalism under fluctuations. Fluctuations can be included in the GENERIC formalism [18,20], resulting in a stochastic differential equation (SDE) of the form

$$\begin{aligned} dz &= \mu(z)dt + \sigma(z)d\mathbf{W}_t, \\ \text{subject to } L(z) \frac{\partial S}{\partial \mathbf{z}}(z) &= \sigma(z) \frac{\partial E}{\partial \mathbf{z}}(z) = \mathbf{0}, \\ L(z) &\text{ is skew-symmetric, i.e., } L(z) = -L(z)^\top, \\ \sigma(z)\sigma(z)^\top &\stackrel{\neq}{=} k_B M(z), \end{aligned} \quad (4.1)$$

where $\mu(z) = L(z) \frac{\partial E}{\partial \mathbf{z}}(z) + M(z) \frac{\partial S}{\partial \mathbf{z}}(z) + k_B \frac{\partial}{\partial \mathbf{z}} \cdot M$, \mathbf{W}_t is a multicomponent Wiener process and k_B is the Boltzmann constant, which controls the magnitude of fluctuation. When the fluctuations are eliminated by letting $k_B \rightarrow 0$, we recover (2.3) from (4.1). Here $\frac{\partial}{\partial \mathbf{z}} \cdot M$ represents the divergence of M as a tensor field, i.e., $\frac{\partial}{\partial \mathbf{z}} \cdot M = \sum_{i=1}^d \sum_{k=1}^d \frac{\partial M_{ik}}{\partial z_k} \mathbf{e}_i$ where \mathbf{e}_i 's are the standard basis vectors in \mathbb{R}^d . The consistency condition of (4.1) implies the conservation of energy and fluctuation-dissipation theorem.

In the stochastic setting, the goal is to infer the drift and diffusion terms μ, σ from observed data. Let $Z(t, \omega; Z_0)$ be the solution to the SDE (4.1), where ω denotes that $Z(t, \omega; Z_0)$ is a random variable and possesses the initial condition $Z(t_0, \omega; Z_0) = Z_0$ with probability one. The data are then referred to N_{traj} sample paths of the solution to (4.1), each of which has different initial states, $\{Z_0^{(k)}\}$, sampled from a probability distribution. The k -th sample path is then written as $\{t_j, \mathbf{z}_j^{(k)}\}_{j=0}^T$ where $\mathbf{z}_j^{(k)} = Z(t_j, \omega^{(k)}; Z_0^{(k)})$ and $\omega^{(k)}$ is a realization of outcome.

GFINNs for the SDE (4.1) consist of the components $A_{\text{NN}}, G_{\text{NN}}, Q_{E_{\text{NN}}}, T_M$ from (3.6) and (3.7), which further construct μ_{NN} and σ_{NN} as follows:

$$\begin{aligned} \mu_{\text{NN}}(z) &= L_{\text{NN}}(z) \frac{\partial E_{\text{NN}}}{\partial \mathbf{z}}(z) + M_{\text{NN}}(z) \frac{\partial S_{\text{NN}}}{\partial \mathbf{z}}(z) + k_B \frac{\partial}{\partial \mathbf{z}} \cdot M_{\text{NN}}(z), \\ \sigma_{\text{NN}}(z) &= \sqrt{2k_B} (T_M(z) Q_{E_{\text{NN}}}(z))^\top. \end{aligned} \quad (4.2)$$

Both $\mu_{\text{NN}}(z)$ and σ_{NN} are naturally defined thanks to the spectral structure of A_{NN} . Since each component obeys the required conditions of (2.3), GFINNs (4.2) satisfy the consistency conditions of (4.1).

Loss function. In the deterministic examples, the loss function is set to the mean squared error (MSE) defined in (2.2) together with the Runge-Kutta second/third order integrator [24].

In the stochastic example, the loss function is set to the negative log-likelihood function (4.3) together with the Euler-Maruyama integrator [32]. The same loss function is also used in [22,33], which is defined by

$$\mathcal{L}(\theta) = -\frac{1}{N_{\text{traj}}} \sum_{k=1}^{N_{\text{traj}}} \frac{1}{T} \sum_{j=1}^T \mathfrak{b} \ p(\mathbf{z}_j^{(k)} | \mathbf{z}_{j-1}^{(k)}, \theta), \quad (4.3)$$

where $p(\mathbf{z}_j^{(k)} | \mathbf{z}_{j-1}^{(k)}, \theta)$ is the probability density function of multivariate normal distribution with mean $\Delta t_j \mu_{\text{NN}}(\mathbf{z}_{j-1}^{(k)})$ and covariance matrix $2k_B \Delta t_j M_{\text{NN}}(\mathbf{z}_{j-1}^{(k)})$ evaluated at $\mathbf{z}_j^{(k)} - \mathbf{z}_{j-1}^{(k)}$. Here $\Delta t_j = t_j - t_{j-1}$.

Evaluation metric. The performance quality of learned dynamics is measured by a closeness between unseen ground truth trajectories that are not used in training, and trajectories of inferred dynamics. This is often referred to as generalization or test error.

Let N_{test} be the number of unseen test trajectories. For $k = 1, \dots, N_{\text{test}}$, let $\mathbf{Z}^{(k)} \in \mathbb{R}^{T \times d}$ be the matrix representing the k -th *unseen* trajectory of ground-truth, whose j -th row, denoted by $\mathbf{Z}_j^{(k)}$, is the state at time t_j . Similarly, let $\tilde{\mathbf{Z}}^{(k)} \in \mathbb{R}^{T \times d}$ be the k -trajectory matrix of learned dynamics whose initial state is the same as the one of $\mathbf{Z}^{(k)}$.

In the deterministic case, the metric we use for closeness is the mean squared error (MSE):

$$\text{MSE}(t_j) = \frac{1}{N_{\text{test}}} \sum_{k=1}^{N_{\text{test}}} \frac{1}{d} \sum_{l=1}^d (\mathbf{z}_{jl}^{(k)} - \tilde{\mathbf{z}}_{jl}^{(k)})^2. \quad (4.4)$$

In the stochastic case, the metric we use for closeness is the squared sliced Wasserstein-2 distance [34], which is defined through random projections. Let $\{\mathbf{u}_m\}_{m=1}^M$ be a set of M vectors randomly uniformly sampled from the unit hypersphere \mathbb{S}^{d-1} , where we set $M = 1000$ for implementation. For each j and m , $\langle \mathbf{z}_j^{(k)}, \mathbf{u}_m \rangle$ and $\langle \tilde{\mathbf{z}}_j^{(k)}, \mathbf{u}_m \rangle$ are always assumed to be sorted with respect to the index k . The squared sliced Wasserstein-2 distance (SW) is then defined by

$$\text{SW}(t_j) = \frac{1}{N_{\text{test}}} \sum_{k=1}^{N_{\text{test}}} \frac{1}{M} \sum_{m=1}^M |\langle \mathbf{z}_j^{(k)} - \tilde{\mathbf{z}}_j^{(k)}, \mathbf{u}_m \rangle|^2.$$

(a) Two gas containers exchanging heat and volume

We consider the gas container example from [35]. Two gas containers are allowed to exchange heat and volume with a wall in the middle. The state variable is $\mathbf{z} = (q, p, S_1, S_2) \in \mathbb{R}^4$, where q, p represent the position and momentum of the moving wall, and S_1, S_2 represent the entropy of the gases in two containers. The energy of the whole system is $E(\mathbf{z}) = \frac{p^2}{2m} + E_1 + E_2$, where $E_i = \left(\frac{e^{S_i/k_B}}{V_i} \right)^{\frac{2}{3}}$, $V_1 = q, V_2 = -q$ and $\hat{c} = \left(\frac{4\pi m}{3h^2 N} \right)^{\frac{3}{2}} \frac{e^{\frac{5}{2}}}{N}$, which follows from the Sackur-Tetrode equation [36] for ideal gases. m is the mass of the wall, N is the number of gas particles, h is the Planck constant and k_B is the Boltzmann constant. We fix the units such that $m = N k_B = c = 1$. The entropy of the system is $S(\mathbf{z}) = S_1 + S_2$. The evolution equation is described by a system of ordinary differential equations (ODEs):

$$\begin{pmatrix} \dot{q} \\ \dot{p} \\ \dot{S}_1 \\ \dot{S}_2 \end{pmatrix} = \begin{pmatrix} \frac{p}{m} \\ \frac{2}{3} \left(\frac{E_1}{q} - \frac{E_2}{-q} \right) \\ \frac{\alpha}{T_1} \left(\frac{1}{T_1} - \frac{1}{T_2} \right) \\ -\frac{\alpha}{T_2} \left(\frac{1}{T_1} - \frac{1}{T_2} \right) \end{pmatrix} = L \frac{\partial E(\mathbf{z})}{\partial \mathbf{z}} + M(\mathbf{z}) \frac{\partial S(\mathbf{z})}{\partial \mathbf{z}}, \quad (4.5)$$

where $L = \begin{bmatrix} S & 0 \\ 0 & 0 \end{bmatrix}$, $M = \begin{bmatrix} 0 & 0 \\ 0 & T \end{bmatrix}$, $S = \begin{bmatrix} 0 & 1 \\ -1 & 0 \end{bmatrix}$, $T = \alpha \begin{bmatrix} T_1^{-2} & -(T_1 T_2)^{-1} \\ -(T_1 T_2)^{-1} & T_2^{-2} \end{bmatrix}$, $T_i = \frac{\partial E_i}{\partial S_i}$, $\mathbf{0}$ is the zero matrix of size 2×2 and α is the parameter determining the strength of heat exchange which we set to 10.

The following proposition shows that the governing equation (4.5) of the gas container problem satisfies all the assumptions of Section 3.

Proposition 1. Let $M(\mathbf{z})$ be the matrix defined in (4.5). Let

$$F_M(\mathbf{z}) = e^{CS_1} q^{-\frac{2}{3}} + e^{CS_2} (-q)^{-\frac{2}{3}},$$

where $C = \frac{2}{3Nk_B}$. Then, $\mathbf{k} M(\mathbf{z}) = \text{span}\{e_1, e_2, \nabla F_M(\mathbf{z})\}$, where

$$\nabla F_M(\mathbf{z}) = (T_3, 0, T_1, T_2)^\top, \quad T_3 = -\frac{2}{3} e^{\frac{2}{3}CS_1} q^{-\frac{5}{3}} + \frac{2}{3} e^{\frac{2}{3}CS_2} (-q)^{-\frac{5}{3}}.$$

Let $\hat{q}(\mathbf{z}) = (0, \bar{T}_1, \bar{T}_2)^\top$ where $\bar{T}_i = \frac{T_i}{\sqrt{T_1^2 + T_2^2}}$. Then, $\{e_1, e_2, \hat{q}(\mathbf{z})\}$ is an orthonormal basis for $\mathbf{k} M(\mathbf{z})$ and $\text{range}(\mathbf{J}\hat{q}(\mathbf{z})^\top) \not\subset \mathbf{k} M(\mathbf{z})$. Furthermore, $E \in \mathcal{F}_M$ as

$$\nabla E(\mathbf{z}) = \mathbf{J}\mathcal{P}_M(\mathbf{z})^\top \mathbf{c}_M \circ \mathcal{P}_M(\mathbf{z}),$$

where $\mathcal{P}_M(\mathbf{z}) = (q, p, F_M(\mathbf{z})^\top, \mathbf{c}_M(\xi_1, \xi_2, \xi_3) = (\xi_2/m, 1)^\top$, and $(\mathbf{J}\mathcal{P}_M(\mathbf{z})^\top)^\top = e_1, e_2, \nabla F_M(\mathbf{z})$.

Proof. The proof directly follows from a straight forward calculation. \square

We use 80 trajectories starting from $t_0 = 0$ to $t_T = 8$ with $\Delta t_j = t_j - t_{j-1} = 0.1$ ($T = 8$) as training data and use another 20 trajectories as test data. The initial conditions of both training and testing trajectories are uniformly sampled from $[0.2, 1.8] \times [-1, 1] \times [1, 1.8] \times [1, 1.8]$. Since neural networks may be sensitive to how parameters are initialized, we run ten independent simulations and report some ensembles out of it. As an effort to make a fair comparison, neural networks used for each method have a roughly similar number of parameters. The detailed architectures are summarized in Table 2 of Appendix A.

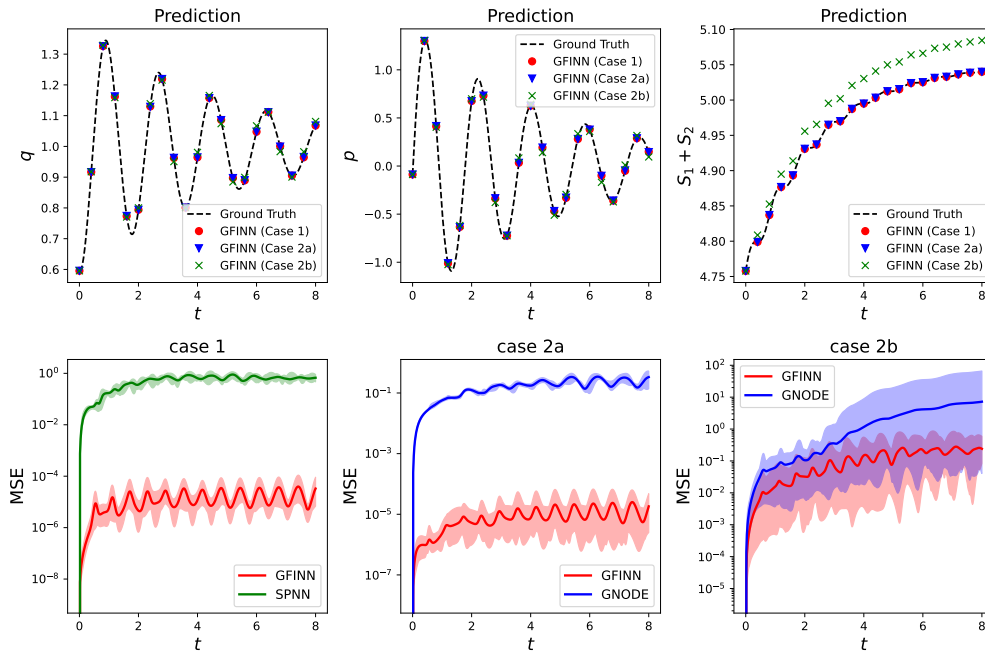


Figure 3. Results for the gas container example. (Top-left and Top-middle) Predicted position q and momentum p for the wall. **(Top-right)** Predicted entropy $S_1 + S_2$ of the air in two gas containers. **(Bottom-left)** The prediction MSE of GFINN and SPNN in case 1. **(Bottom-middle and bottom-right)** The prediction MSE of GFINN and GNODE in case 2a and case 2b. The results are obtained by taking the mean of 10 simulations, while the upper and lower boundary for shaded region represents the highest and lowest error in 10 simulations.

In the top row of Figure 3, we plot one of 20 test trajectories as dashed-lines, together with the corresponding trajectory of the learned dynamics by GFINNs as symbols; the circle (\circ), the inverted triangle (∇) and the cross (\times) marks correspond to case 1, case 2a and case 2b, respectively. Here, GFINNs are the one with the smallest MSE summed over time among 10 simulations. Since the state variable lies in \mathbb{R}^4 , the q , p and $S_1 + S_2$ trajectories are reported. We clearly see that in case 1 and case 2a, the trajectories of GFINNs are indistinguishable to the ground truth trajectory, while in case 2b, they start to deviate from the truth trajectory as time increases. This is expected as some underlying physics in terms of the GENERIC formalism is known in case 1 and case 2a, while no physics is known in case 2b.

To compare against other methods, in the bottom row of Figure 3, we report the means of the MSE (4.4) of GFINNs, GNODEs and SPNNs with respect to time. Each shaded region represents the range between the maximum and the minimum of the MSEs from ten simulations. We clearly observe that the mean of the MSEs by GFINNs is much lower than those by SPNNs and GNODEs in all the cases. In both case 1 and case 2a, all the 10 MSEs of GFINNs are significantly lower than those of the other comparisons. This again demonstrates that by incorporating physical

knowledge into neural networks, GFINNs can achieve much higher predictive accuracy. In case 2b, the mean MSE of GFINNs is at least one order magnitude smaller than the one of GNODEs in almost all times. These results indicate that to achieve good performance, it is not enough to just enforce the GENERIC conditions, but a sufficient expressivity is also required to capture the underlying dynamics.

In Figure 4, we plot the contours of energy and entropy functions from both the ground truth and GFINNs in all the cases. Due to the nonuniqueness of the GENERIC formalism, a proper calibration is applied. We see that the calibrated contours of both the energy and entropy by GFINNs are indistinguishable to those by the ground truth. This demonstrates the discovery of the energy and entropy by GFINNs from data.

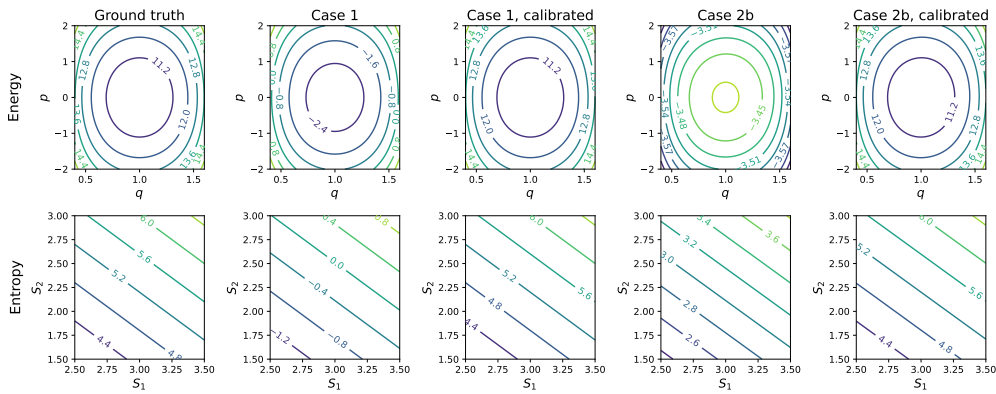


Figure 4. Learned energy E and entropy S of the gas container example by GFINN. In both case 1 and case 2b, the GFINNs can recover the correct energy and entropy of the system when the undetermined scaling and translation factor is calibrated with the ground truth. We show the energy surface at the hyperplane $\{z : S_1 = 2.5, S_2 = 2.5\}$ as a function of p, q and the entropy surface at $\{z : p = 0, q = 1\}$ as a function of S_1 and S_2 .

(b) Thermoelastic double pendulum

We consider the two-dimensional finite thermoelastic double pendulum example [37]. The state variable is $z \in (q_1, q_2, p_1, p_2, S_1, S_2) \in \mathbb{R}^{10}$, where $q_i, p_i \in \mathbb{R}^2$ represent the position, momentum of the i -th mass, and S_i represents the entropy of the i -th spring. We denote the length of two springs as $\lambda_1 = \|q_1\|, \lambda_2 = \|q_2 - q_1\|$. The total energy of the system is $E(z) = \frac{\|p_1\|^2}{2} + \frac{\|p_2\|^2}{2} + E_1 + E_2$, where E_1 and E_2 are the internal energy of both springs, defined by $E_i = \frac{1}{2}k(\lambda_i)^2 + k\lambda_i + e^{S_i - \log \lambda_i} - 1$. The entropy of the system is $S(z) = S_1 + S_2$. The evolution equation for the problem is then given by a system of ODEs:

$$\begin{pmatrix} \dot{q}_1 \\ \dot{q}_2 \\ \dot{p}_1 \\ \dot{p}_2 \\ \dot{S}_1 \\ \dot{S}_2 \end{pmatrix} = \begin{pmatrix} p_1 \\ p_2 \\ -\frac{\partial}{\partial q_1}(E_1 + E_2) \\ -\frac{\partial}{\partial q_2}(E_1 + E_2) \\ T_1^{-1}T_2 - 1 \\ T_1T_2^{-1} - 1 \end{pmatrix} = L \frac{\partial E(z)}{\partial z} + M(z) \frac{\partial S(z)}{\partial z}, \quad (4.6)$$

where $T_i = \frac{\partial E_i}{\partial S_i}$, $\mathbf{0}$ and $\mathbf{1}$ are 2×2 matrices whose elements are all 0 and 1, respectively, $\mathbf{0}_{m_1 \times m_2}$ is a matrix of size $m_1 \times m_2$ whose elements are all 0,

$$L = \begin{pmatrix} \mathbf{0}_{4 \times 4} & \mathbf{S} \\ -\mathbf{S}^\top & \mathbf{0}_{6 \times 6} \end{pmatrix}, \quad M(\mathbf{z}) = \begin{pmatrix} \mathbf{0}_{8 \times 8} & \mathbf{0}_{8 \times 2} \\ \mathbf{0}_{2 \times 8} & \mathbf{T}(\mathbf{z}) \end{pmatrix}, \quad \mathbf{S} = \begin{pmatrix} \mathbf{1} & \mathbf{0} & \mathbf{0} \\ \mathbf{0} & \mathbf{1} & \mathbf{0} \end{pmatrix}, \quad \mathbf{T} = \begin{pmatrix} \frac{T_2}{T_1} & -1 \\ -1 & \frac{T_1}{T_2} \end{pmatrix}. \quad (4.7)$$

The governing equation (4.6) for the problem again satisfies all the assumptions in Section 3, which is shown in the following proposition.

Proposition 2. Let $M(\mathbf{z})$ be the matrix defined in (4.7). Let $F_M(\mathbf{z}) = -\|\mathbf{q}_1\|e^{S_1} - \|\mathbf{q}_2 - \mathbf{q}_1\|e^{S_2}$. Then, $\mathbf{K} M(\mathbf{z}) = \text{span}\{e_1, \dots, e_8, \nabla F_M(\mathbf{z})\}$ and $\nabla F_M(\mathbf{z}) \in \text{range}(T_3; T_4; \mathbf{0}_{4 \times 1}; T_1; T_2)$ where

$$T_3 = -\frac{\mathbf{q}_1}{\|\mathbf{q}_1\|}e^{S_1} + \frac{\mathbf{q}_2 - \mathbf{q}_1}{\|\mathbf{q}_2 - \mathbf{q}_1\|}e^{S_2}, \quad T_4 = -\frac{\mathbf{q}_2 - \mathbf{q}_1}{\|\mathbf{q}_2 - \mathbf{q}_1\|}e^{S_2}.$$

Let $\hat{\mathbf{q}}(\mathbf{z}) \in \mathbf{0}_{8 \times 1}; \bar{T}_1; \bar{T}_2$ where $\bar{T}_i = \frac{T_i}{\sqrt{T_1^2 + T_2^2}}$. Then, $\{e_1, \dots, e_8, \hat{\mathbf{q}}(\mathbf{z})\}$ is an orthonormal basis for $\mathbf{K} M(\mathbf{z})$ and $\text{range}(\mathbf{J}\hat{\mathbf{q}}(\mathbf{z})^\top) \not\subset \mathbf{K} M(\mathbf{z})$. Furthermore, $E \in \mathcal{F}_M$ and $\nabla E(\mathbf{z}) \in \mathbf{JP}_M(\mathbf{z})^\top \mathbf{c}_M \circ \mathcal{P}_M(\mathbf{z})$, where $\mathcal{P}_M(\mathbf{z}) \in \mathbf{q}_1, \mathbf{q}_2, \mathbf{p}_1, \mathbf{p}_2, F_M(\mathbf{z})^\top, \mathbf{c}_M(\xi) \in \mathbf{0}_{4 \times 1}; \xi_5; \dots; \xi_8$ and $(\mathbf{JP}_M(\mathbf{z}))^\top = [e_1, \dots, e_8, \nabla F_M(\mathbf{z})]$.

Proof. The proof directly follows from a straight forward calculation. \square

We generate 100 trajectories from $t_0 \in [0, 1]$ to $t_T \in [0, 1]$ with $\Delta t \in [0.1, 0.2]$ ($T \in [0.1, 0.2]$), whose initial conditions are sampled uniformly from $[0.9, 1] \times [-0.1, 0] \times [0.1, 2] \times [-0.1, 0] \times [-0.1, 0] \times [0.9, 2] \times [0.9, 1] \times [-0.1, 0] \times [0.9, 1] \times [0.1, 0.3]$. We use 80 of them for training and the remaining for testing.

In the top row of Fig 5, we again plot one of 20 test trajectories, together with the predicted trajectories of GFINNs in the same way as in the previous example. Since the state variable lies in \mathbb{R}^{10} , we plot the predicted trajectories of λ_1, λ_2 and $S_1 + S_2$. We see that the predicted length and entropy of the springs by GFINNs match the ground truth in case 1 and case 2a. In case 2b, due to the chaotic nature of the problem, the predicted trajectory starts to deviate from the ground after certain time.

In the bottom row of Fig 5, we report the mean MSE of GFINN, SPNNs and GNODEs from ten simulations. The shaded areas indicate the maximum and minimum of MSEs as in the gas container example. We clearly observe that in all cases GFINNs can produce better predictive performance compared to other baseline methods. In case 1, all the 10 MSEs of GFINNs are significantly smaller than those of SPNNs. In case 2a and case 2b, the mean MSE of GFINNs is approximately one order of magnitude smaller than GNODEs most of the time. The only exception is in the time window $t \in [0.5, 0.6]$, when the MSEs for GFINNs and GNODEs become similar.

(c) Langevin equation

We consider the diffusion of a particle described by the Langevin equation. The state variable vector is $\mathbf{z} \in (q, p, S_e) \in \mathbb{R}^3$, where q, p are the position and momentum of the particle, respectively, and S_e is the entropy of the surrounding environment. A simple form of energy and entropy is assumed: $E = \frac{p^2}{2} + S_e$ and $S = S_e$. The Langevin equation is then given by (4.1) with

$$L = \begin{pmatrix} 0 & 1 & 0 \\ -1 & 0 & 0 \\ 0 & 0 & 0 \end{pmatrix}, \quad M(\mathbf{z}) = \begin{pmatrix} 0 & 0 & 0 \\ 0 & \frac{1}{2} & -\frac{p}{2} \\ 0 & -\frac{p}{2} & \frac{p^2}{2} \end{pmatrix}, \quad \sigma(\mathbf{z}) = \begin{pmatrix} 0 \\ 1 \\ -p \end{pmatrix}. \quad (4.8)$$

Note that we choose units such that $k_B = 1$ for notational simplicity.

We simulate 40 trajectories between $t_0 \in [0, 1]$ to $t_T \in [0, 1]$ with $\Delta t \in [0.1, 0.2]$ for training. The initial state is randomly sampled from a normal distribution with mean $[0, 2, 0]^\top$ and covariance matrix

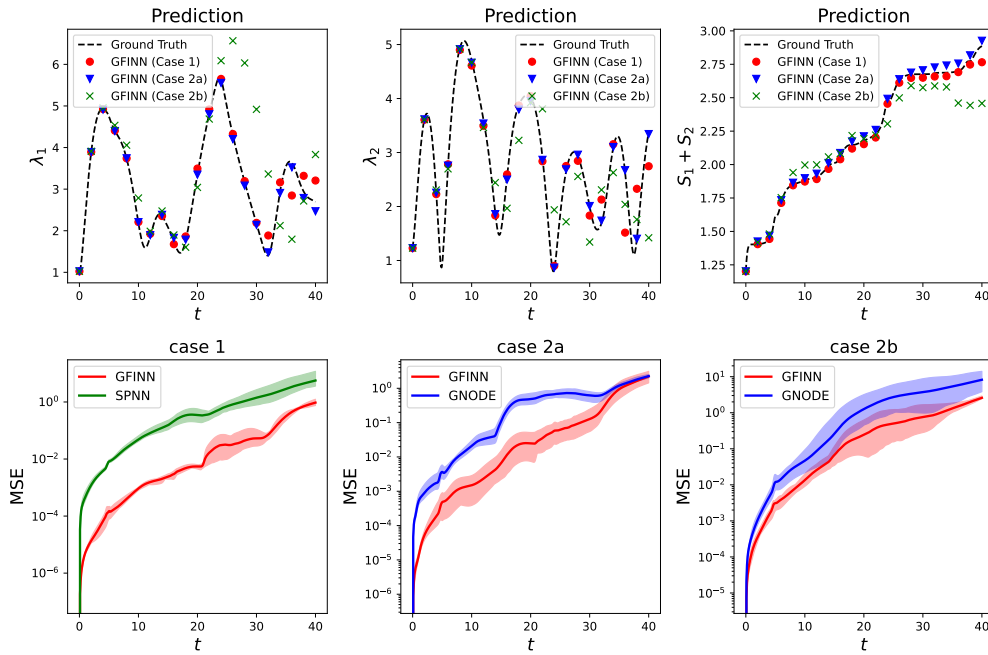


Figure 5. Results for the thermoelastic double pendulum example. (Top) Predicted length of springs λ_1 , λ_2 and the predicted total entropy $S_1 + S_2$. Better predictive performance is achieved when there is additional physical knowledge (case 1 and case 2a) beyond the GENERIC formalism. **(Bottom)** The MSE of GFINNs, SPNNs and GNODEs. By incorporating hard constraints into the neural network, GFINNs can produce better predictive performances compared to SPNNs and GNODEs.

$0.4^2 I$, where I is the identity matrix of size 3. To evaluate the predictive performance of the model, we sample another 50,000 initial conditions from the same distribution, and solve (4.1) using both the ground truth μ, σ and inferred $\mu_{\text{NN}}, \sigma_{\text{NN}}$ with the Euler-Maruyama method. Then we apply the Gaussian kernel density estimator [38] to approximate the distribution of z and z_{NN} at time steps $t \in \{0, 0.5, 1, 2\}$, results of which can be found in Fig. 6. Note that we infer dynamics from stochastic samples. In case 1 and case 2a, our model is not only able to recover the correct distribution of $z(t)$, but also gives the correct prediction when extrapolating in time ($t \notin \{0, 0.5, 1, 2\}$), using a small amount of data. However, for case 2b and SDENet, even though a similar training error is achieved as shown in Table 1, the predicted trajectories do not match the ground truth, which indicates that prior physical knowledge is crucial to make the data-efficient inference. Still, the prediction error of GFINNs is smaller than that of SDENets in all cases as shown in Table 1.

	Case 1	Case 2a	Case 2b	SDENet
Training loss	-2.7856	-2.7844	-2.6910	-2.7690
Prediction error, $t \in \{0, 0.5, 1, 2\}$	1.3×10^{-2}	4.6×10^{-4}	7.6×10^{-2}	4.0×10^{-1}
Prediction error, $t \notin \{0, 0.5, 1, 2\}$	6.7×10^{-2}	7.4×10^{-4}	7.4×10^{-1}	1.1

Table 1. Training loss (negative log-likelihood) and prediction error (squared sliced Wasserstein-2 distance) of GFINNs. Even though the training losses of the three cases are similar, the prediction error shows significant differences, which reflects the different generalization capabilities of different models. In all cases, GFINNs produce a lower prediction error compared to SDENets.

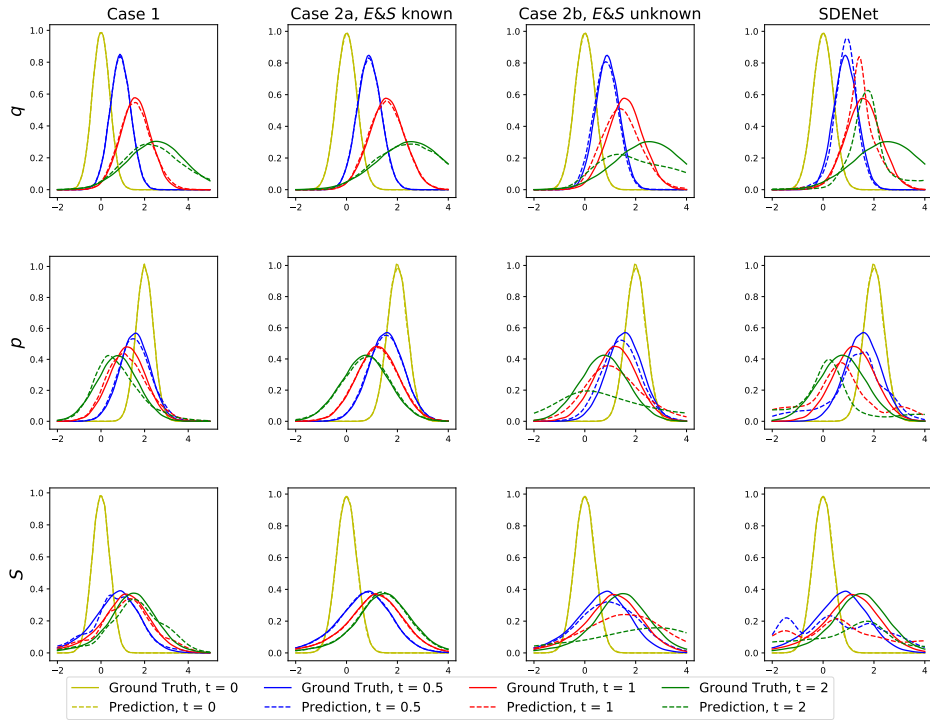


Figure 6. Results for the Langevin equation example. We plot the predicted and true probability distribution of $\mathbf{z}(t)$ at $t = 0, 0.5, 1, 2$ using both types of GFINNs. In case 2a, GFINNs can recover the correct distribution and give the correct prediction when extrapolating in time ($t = 2$). In case 1, there is a small discrepancy between the predicted and true distribution. For case 2b and SDENet, the prediction deviates from the ground truth after certain time.

A. Implementation of architecture

(a) GNODEs

The GNODEs [23] parameterize L, M based on bracket structure and use standard neural networks for modelling E, S . The GNODEs' architecture is designed for case 2b and their architecture has a similarity with GFINNs in that two independent neural networks $E_{\text{NN}}, S_{\text{NN}}$ are used to parameterize E and S . However, a key difference lies in the network architectures for L and M . Specifically, GNODEs model L and M by L^{GNODE} and M^{GNODE} whose (α, β) components are defined by

$$L_{\alpha\beta}^{\text{GNODE}}(\mathbf{z}) = \sum_{\gamma} \xi_{\alpha\beta\gamma} \nabla S_{\text{NN}}(\mathbf{z})_{\gamma}, \quad M_{\alpha\beta}^{\text{GNODE}}(\mathbf{z}) = \sum_{\mu, \nu, m, n} A_{\alpha\beta}^m D_{mn} A_{\mu\nu}^n \nabla E_{\text{NN}}(\mathbf{z})_{\beta} \nabla E_{\text{NN}}(\mathbf{z})_{\nu}$$

where ξ is a 3d skew-symmetric tensor, A^m are 2d skew-symmetric matrices, D is a positive semi-definite matrix. Due to the bracket structure, the GENERIC conditions are enforced under such parameterization. However, L^{GNODE} and M^{GNODE} are merely functions of $\nabla S_{\text{NN}}(\mathbf{z})$ and $\nabla E_{\text{NN}}(\mathbf{z})$ respectively, which can be seen as the underlying model assumption that differs from GFINNs. In examples where such assumption holds, GNODEs may achieve good performance because they incorporate stronger physical prior knowledge. However, when A depends on not only $\nabla G(\mathbf{z})$ but also on some other functions of \mathbf{z} , GNODEs cannot represent the underlying governing equations due to the lack of expressivity. In [23], the mean squared error (2.2) is also used as the loss function.

(b) SPNNs

[15] proposed SPNNs, which parameterize the gradient of the energy and entropy assuming L and M are known (case 1). The loss function for SPNNs is defined as

$$\mathcal{L}(\theta) = \frac{1}{N_{\text{traj}}} \sum_{k=1}^{N_{\text{traj}}} \frac{1}{T} \sum_{j=1}^T \left(\left\| z_{\text{NN}}(t_j; z_0^{(k)}; \theta) - z(t_j; z_0^{(k)}) \right\|^2 + \lambda \left(\|L(dS)_{\text{NN}}\|^2 + \|M(dE)_{\text{NN}}\|^2 \right) \right),$$

where $(dE)_{\text{NN}}$ and $(dS)_{\text{NN}}$ are standard feed-forward neural networks (FNNs) parameterizing ∇E and ∇S , $L(dS)_{\text{NN}}$ and $M(dE)_{\text{NN}}$ are both evaluated at $z(t_j; z_0^{(k)})$, λ is the hyperparameter which controls the scale of the soft penalty, and $z_{\text{NN}}(t_j; z_0^{(k)}; \theta)$ is computed by applying a numerical integrator to the equation $\dot{z}(t) = F_{\text{NN}}(z; \theta) = L(z) \nabla E_{\text{NN}}(z) + M(z) \nabla S_{\text{NN}}(z)$ starting at $z(t_{j-1}; z_0^{(k)})$.

However, the architecture we used for comparison is slightly different from that in the original paper, i.e., we model E, S instead of ∇E and ∇S as neural networks. By parameterizing E, S as neural networks, the surrogate model can learn a dynamical system more effectively, due to the inductive bias that ∇E and ∇S should satisfy the Clairaut's theorem. Another reason for our choice is that we parameterize E, S as neural networks in GFNNs, and the comparison should be made fair by control of variables.

In this paper we choose λ from $\{0.0, 0.1, 1\}$ and pick the ones that give the lowest MSEs in the two deterministic problems.

(c) SDENet

The SDENets parameterize the drift and diffusion term μ and σ as two independent FNNs and use the negative log-likelihood function (4.3) as the loss function.

Problem		Gas container		Double pendulum		Langevin equation		
		GFINN	GNODE	GFINN	GNODE	GFINN	SDENet	
Layers	L	-/5/5	-	-/5/5	-	-/5/5	μ	5
	M	-/5/5	-	-/5/5	-	-/5/1		
	E	5/-/5	5	5/-/5	5	5/-/5	σ	5
	S	5/-/1	1	5/-/5	5	5/-/1		
Width	L	-/30/30	-	-/30/30	-	-/30/30	μ	30
	M	-/30/30	-	-/30/30	-	-/30/-		
	E	30/-/30	30	30/-/30	30	30/-/30	σ	30
	S	30/-/-	-	30/-/30	30	30/-/-		

Table 2. Model architecture. The number of layers and width of the neural network is slightly different across three cases considered in the paper (case 1, case 2a and case 2b). We list all of them in the table separated by the slash. The layers and width for each component of SPNNs is set to be the same as GFNNs. The hyperbolic tangent (tanh) activation functions are used for all the models. The optimizer is chosen to be Adam [39] with learning rate 0.001. For the gas container and double pendulum examples, we train the models using mini-batch with batch size 100 for 5×10^5 iterations. For the Langevin equation example, we train the models using full batch for 5×10^4 iterations. The important dimension K of skew-symmetric matrices $Q_{S_{\text{NN}}}(z)$ and $Q_{E_{\text{NN}}}(z)$ in the parameterization of L_{NN} and M_{NN} are chosen to be 5 and 4 respectively in all examples.

Acknowledgments

We would like to acknowledge the support by DOE PhILMs (no. DE-SC0019453) and OSD/AFOSR MURI grant FA9550-20-1-0358. We would like to acknowledge the helpful discussion with Dr.

Xin Bian, Dr. Zhen Li and Dr. Chensen Lin. We would like to thank Dr. Kookjin Lee, Dr. Nat Trask and Dr. Panos Stinis for providing the codes of the GNODE paper.

References

1. Bongard J, Lipson H. 2007 Automated reverse engineering of nonlinear dynamical systems. *Proceedings of the National Academy of Sciences* **104**, 9943–9948.
2. Brunton SL, Proctor JL, Kutz JN. 2016 Discovering governing equations from data by sparse identification of nonlinear dynamical systems. *Proceedings of the national academy of sciences* **113**, 3932–3937.
3. Schmidt M, Lipson H. 2009 Distilling free-form natural laws from experimental data. *science* **324**, 81–85.
4. Chang B, Meng L, Haber E, Ruthotto L, Begert D, Holtham E. 2017 Reversible architectures for arbitrarily deep residual neural networks. *arXiv preprint arXiv:1709.03698*.
5. E W. 2017 A proposal on machine learning via dynamical systems. *Communications in Mathematics and Statistics* **5**, 1–11.
6. Haber E, Ruthotto L. 2017 Stable architectures for deep neural networks. *Inverse Problems* **34**, 014004.
7. Lu Y, Zhong A, Li Q, Dong B. 2018 Beyond finite layer neural networks: Bridging deep architectures and numerical differential equations. In *International Conference on Machine Learning* pp. 3276–3285. PMLR.
8. Qin T, Wu K, Xiu D. 2019 Data driven governing equations approximation using deep neural networks. *Journal of Computational Physics* **395**, 620–635.
9. Raissi M, Perdikaris P, Karniadakis GE. 2018 Multistep neural networks for data-driven discovery of nonlinear dynamical systems. *arXiv preprint arXiv:1801.01236*.
10. Chen TQ, Rubanova Y, Bettencourt J, Duvenaud DK. 2018 Neural Ordinary Differential Equations. In *NeurIPS* pp. 6572–6583.
11. Kidger P, Morrill J, Foster J, Lyons TJ. 2020 Neural Controlled Differential Equations for Irregular Time Series. In *NeurIPS*.
12. Greydanus S, Dzamba M, Yosinski J. 2019 Hamiltonian Neural Networks. In Wallach H, Larochelle H, Beygelzimer A, d'Alché-Buc F, Fox E, Garnett R, editors, *Advances in Neural Information Processing Systems* vol. 32. Curran Associates, Inc.
13. Raissi M, Perdikaris P, Karniadakis GE. 2019 Physics-informed neural networks: A deep learning framework for solving forward and inverse problems involving nonlinear partial differential equations. *Journal of Computational Physics* **378**, 686–707.
14. Cranmer M, Greydanus S, Hoyer S, Battaglia P, Spergel D, Ho S. 2020 Lagrangian Neural Networks. In *ICLR 2020 Workshop on Integration of Deep Neural Models and Differential Equations*.
15. Hernández Q, Badías A, González D, Chinesta F, Cueto E. 2021 Structure-preserving neural networks. *Journal of Computational Physics* **426**, 109950.
16. Jin P, Zhang Z, Kevrekidis IG, Karniadakis GE. 2020a Learning Poisson systems and trajectories of autonomous systems via Poisson neural networks. *arXiv preprint arXiv:2012.03133*.
17. Jin P, Zhang Z, Zhu A, Tang Y, Karniadakis GE. 2020b SympNets: Intrinsic structure-preserving symplectic networks for identifying Hamiltonian systems. *Neural Networks* **132**, 166–179.
18. Grmela M, Öttinger HC. 1997 Dynamics and thermodynamics of complex fluids. I. Development of a general formalism. *Physical Review E* **56**, 6620.
19. Öttinger HC, Grmela M. 1997 Dynamics and thermodynamics of complex fluids. II. Illustrations of a general formalism. *Physical Review E* **56**, 6633.
20. Öttinger HC. 2005 *Beyond equilibrium thermodynamics*. John Wiley & Sons.
21. Trefethen LN, Bau DI. 1997 *Numerical linear algebra* vol. 50. Siam.
22. Dietrich F, Makeev A, Kevrekidis G, Evangelou N, Bertalan T, Reich S, Kevrekidis IG. 2021 Learning effective stochastic differential equations from microscopic simulations: combining stochastic numerics and deep learning. *arXiv preprint arXiv:2106.09004*.
23. Lee K, Trask NA, Stinis P. 2021 Machine learning structure preserving brackets for forecasting irreversible processes. *arXiv preprint arXiv:2106.12619*.
24. Lambert JD. 1991 *Numerical methods for ordinary differential systems* vol. 146. Wiley New York.
25. Cybenko G. 1989 Approximation by superpositions of a sigmoidal function. *Math. Control Signal* **2**, 303–314.

26. Siegel JW, Xu J. 2020 Approximation rates for neural networks with general activation functions. *Neural Networks* **128**, 313–321.
27. Mhaskar HN. 1996 Neural networks for optimal approximation of smooth and analytic functions. *Neural computation* **8**, 164–177.
28. Paszke A, Gross S, Massa F, Lerer A, Bradbury J, Chanan G, Killeen T, Lin Z, Gimelshein N, Antiga L et al.. 2019 Pytorch: An imperative style, high-performance deep learning library. *Advances in neural information processing systems* **32**, 8026–8037.
29. Abadi M, Barham P, Chen J, Chen Z, Davis A, Dean J, Devin M, Ghemawat S, Irving G, Isard M et al.. 2016 Tensorflow: A system for large-scale machine learning. In *12th {USENIX} symposium on operating systems design and implementation ({OSDI} 16)* pp. 265–283.
30. Golub GH, Pereyra V. 1973 The differentiation of pseudo-inverses and nonlinear least squares problems whose variables separate. *SIAM Journal on numerical analysis* **10**, 413–432.
31. Li X. 1996 Simultaneous approximations of multivariate functions and their derivatives by neural networks with one hidden layer. *Neurocomputing* **12**, 327–343.
32. Kloeden PE, Platen E. 1992 Stochastic differential equations. In *Numerical Solution of Stochastic Differential Equations* pp. 103–160. Springer.
33. Schneider G, Craigmile PF, Herbei R. 2014 Maximum likelihood estimation for stochastic differential equations using sequential kriging-based optimization. *arXiv preprint arXiv:1408.2441*.
34. Deshpande I, Zhang Z, Schwing AG. 2018 Generative modeling using the sliced wasserstein distance. In *Proceedings of the IEEE conference on computer vision and pattern recognition* pp. 3483–3491.
35. Shang X, Öttinger HC. 2020 Structure-preserving integrators for dissipative systems based on reversible–irreversible splitting. *Proceedings of the Royal Society A* **476**, 20190446.
36. Schroeder DV. 1999 An introduction to thermal physics. .
37. Romero I. 2009 Thermodynamically consistent time-stepping algorithms for non-linear thermomechanical systems. *International journal for numerical methods in engineering* **79**, 706–732.
38. Parzen E. 1962 On estimation of a probability density function and mode. *The annals of mathematical statistics* **33**, 1065–1076.
39. Kingma DP, Ba J. 2015 Adam: A Method for Stochastic Optimization. In *3rd International Conference on Learning Representations, ICLR 2015, San Diego, CA, USA, May 7-9, 2015, Conference Track Proceedings*.